Optics Letters

Optical dynamic memory based on an integrated active ring resonator

Jiejun Zhang,[1] Robert S. Guzzon,[2] Larry A. Coldren,[2] and Jianping Yao[1,*]

[1]Microwave Photonics Research Laboratory, University of Ottawa, Ottawa, Ontario K1N 6N5, Canada
[2]Department of Electrical and Computer Engineering, University of California Santa Barbara, Santa Barbara, California 93116, USA
*Corresponding author: jpyao@eecs.uottawa.ca

Received 5 July 2018; revised 15 August 2018; accepted 16 August 2018; posted 27 August 2018 (Doc. ID 337960); published 21 September 2018

All-optical computing has been considered a solution for future computers to overcome the speed bottleneck encountered by the current electronic computers. High-speed optical memory is one of the key building blocks in realizing all-optical computing. In this Letter, we demonstrate an optical dynamic memory based on an amplified high *Q*-factor ring resonator that has the capability to achieve an infinite memory time. The optical memory uses an external pulse train to refresh the resonator, an operation in analogy to an electronic dynamic random-access memory widely used in modern computers, but at a speed that can be orders of magnitude faster. In our demonstration, a writing speed of 2.5 GHz is achieved with instant reading capability. The maximum writing speed can be as fast as 27.3 GHz if a shorter pulse is used.

OCIS codes: (210.4680) Optical memories; (200.4490) Optical buffers; (230.5750) Resonators; (250.4390) Nonlinear optics, integrated optics.

https://doi.org/10.1364/OL.43.004687

High-speed optical memory is one of the key building blocks for all-optical computing [1,2]. Commercial optical storage discs are playing an important role in cost-effective data storage. For example, a Blu-ray disc can store up to 25 gigabytes of data with single-layer patterning [3]. Recent advancements in data writing and storage techniques indicate a potential storage capacity of tens of terabytes per disk, making optical storage a strong competitor in the era of big data [4–6]. In contrast to the optical static memory based on disc patterning, optical dynamic memories that store photons to represent information have the potential of achieving much higher speeds for data reading, writing, and addressing. A high *Q*-factor optical resonator that can trap photons for a long time can be exploited to implement a dynamic optical memory. For example, an optical resonator with a *Q*-factor of 10^8 or higher can provide a photon storage time up to tens of nanoseconds [7]. However, the stored photons will eventually vanish due to the unavoidable loss in a resonator. Integrated amplifiers can be used in an optical resonator to partially compensate for the loss and to increase the photon storage time [7–9]. However, the photon storage time still cannot be infinitely long, since the net gain in the resonator must be strictly less than unity to avoid lasing, making optical memories incompetent for all-optical computation.

Currently, dynamic optical memories are generally implemented with optical bistability devices, which can achieve ultrafast read and write speed, as well as an infinite optical memory time [10–14]. Bistability optical memory can be switched between two output states by an optical control signal, with each state representing an optical logic. For example, an integrated optical memory based on optical bistability was reported in Ref. [13], in which an optical memory was realized by using an optical signal to switch the lasing direction of two microring lasers. The optical memory features an ultrashort switching time of 20 ps and a switching energy of 5.5 fJ. However, a constant optical probe is required for an optical bistability memory to both read the stored data and lock the memory in a specific memory state, which may result in high power consumption. In addition, electrical injection is generally required to sustain the stored optical signal.

In this Letter, we propose and experimentally demonstrate an optical memory based on an integrated active ring resonator that is optically refreshable. To achieve an extended memory time, a refreshing optical pulse that is in-phase with the stored signal is injected into the ring resonator to periodically refresh the stored information. The stored signal can be erased by injecting an optical pulse that is out of phase with the stored signal. The proposed optical memory integrates the merits of those based on a high *Q*-factor resonator with optical bistability, but without the need for a constant probe light. In contrast, a pulsed refreshing signal is used to periodically refresh the stored information, which can potentially have lower power consumption with an infinite memory time. The operation of the memory unit is in analogy to a dynamic random-access memory unit that is widely used in modern computers, in which a capacitor is used to store electrons that are refreshed electrically and periodically. In the proposed memory, information is carried by photons trapped in a resonator, in contrast to conventional optical memories based on optical bistability. The photons can carry more information encoded in polarization, wavelength, phase, and angular momentum and, thus, can potentially enhance the capability for all-optical computing.

Figure 1(a) shows the schematic of the proposed optical memory, and Figs. 1(b)–1(e) show the microscopic image of the fabricated chip which is wire-bonded to a carrier to facilitate electrical connection, and the scanning electron microscope (SEM) images of the key elements in the ring resonator. Four semiconductor optical amplifiers (SOA1-4) are incorporated to compensate for the coupling loss for the input signal, the refreshing signal, and the read-out signal, respectively. To enable a long memory time with a single refresh, two other SOAs (SOA5 and SOA6) are incorporated in the ring resonator to compensate for the round-trip loss. Two tunable couplers (TCs1-2) are used to change the coupling ratios between the bypass waveguides and the ring resonator. Each of the TCs consists of two multimode interferometer (MMI) couplers, and two phase modulators (PMs), as shown in Fig. 1. The coupling ratio of a TC can be tuned from 0 to 100% by changing the driving current that is applied to one of the PMs. The PM located in the ring modulator can be used to tune the resonance wavelength by applying a driving current.

A ring resonator can be used as an optical integrator. The transfer function of an optical integrator is given by [15]

$$H(\omega) = \frac{1}{j(\omega - \omega_0)}, \tag{1}$$

where $j = \sqrt{-1}$, ω is the angular frequency of the input signal, and ω_0 is the optical carrier frequency. An integrator is a band-pass filter with a π-phase jump at its central frequency. The integration of a positive pulse and a negative pulse can erase the information that is encoded in one of the two pulses. A ring resonator can be used to emulate an integrator with a finite integration time window due to its limited Q-factor. Based on the active ring resonator shown in Fig. 1, an optical integrator can be implemented by injecting a signal to be integrated from Port 1 and to get an integrated signal from Port 2. The response of the ring resonator is given by [16]

$$\frac{E_2}{E_1} = \frac{-\kappa_1^* \kappa_2 \sqrt[4]{A} e^{j\phi/2}}{1 - \sqrt{A} t_1^* t_2^* e^{j\phi}}, \tag{2}$$

where t_1, κ_1, and t_2, and κ_2 are the straight-through and cross-over coupling coefficients of TC1 and TC2, respectively; A is the round-trip optical power loss; ϕ is the round-trip optical phase shift given by $\phi = \beta L$, in which β is the propagation constant of the waveguide; and L is the length of the ring resonator. By choosing proper coupling ratios of the TCs and reducing the round-trip loss, the response of a ring resonator can be configured to be close to that of an optical integrator within its free spectral range (FSR). The central wavelength of the integrator is equal to a resonance wavelength of the ring resonator, and the bandwidth is determined by the Q-factor of the ring resonator.

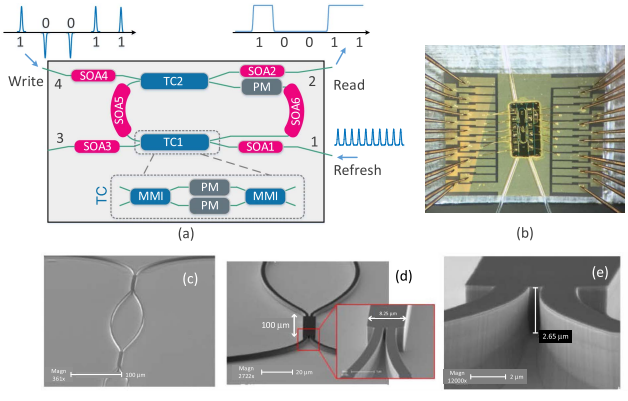

Fig. 1. (a) Schematic of the optical memory unit; (b) a photograph of the optical memory based on the InP/InGaAsP material system, wire-bonded to a polychlorinated biphenyl carrier; (c)–(e) SEM images of the TC, the MMI, and the waveguides. SOA, semiconductor optical amplifier; TC, tunable coupler; PM, phase modulator.

In our implementation, an optical pulse train with a central wavelength λ_c slightly shorter than a resonance wavelength of the ring resonator is launched via Port 1 as a refreshing signal. Due to a wavelength mismatch, the optical pulse train will be blocked from passing through Port 2. In this case, the ring resonator is considered to store an optical logic of "0." To write an optical logic of "1" into the optical memory, an optical pulse with the same phase and a higher energy is launched via Port 4. The writing pulse is split into two parts by TC2, with most of the energy directed to Port 2 and the remaining coupled into the ring resonator. Due to the strong nonlinearity of the SOAs and the PM in the ring resonator, the coupled light will modify the resonance wavelength of the ring modulator [17] so that it will be shifted to λ_c. As a result, the ring resonator works as an integrator for the refreshing signal injected from Port 1. The output signals at Port 2 will be at a high optical power level, which is a sawtooth waveform corresponding to the integration of the refreshing pulse train. The optical memory is switched from optical logic "0" to "1." However, due to the round-trip loss of the ring resonator, a single pulse in the refreshing pulse train can only sustain a high power level at Port 2 for a limited time. Thanks to the use of a pulse train as a refreshing signal, the next pulse will arrive and refresh the pulse recirculating in the resonator before it decays, thus extending the memory time for optical logic "1." In addition, as a high optical power is confined within the ring resonator for "1," the resonance of the ring resonator can be at around λ_c so that the refreshing pulse train can be continuously injected in the ring resonator, to make the resonator remain functioning as an integrator.

In the presence of strong nonlinearity, the internal electrical field is related to the injected optical electrical field E_1 [10]:

$$E_{\text{internal}} = \frac{\kappa_1 E_1}{1 - t_1^2 e^{2ikl - al}}, \tag{3}$$

where k and α are the optical-intensity-dependent refractive index and loss of the ring resonator, respectively. The refreshing pulse train can only be injected into the ring resonator when there is already an optical signal recirculating in it, which shifts the resonance wavelength of the ring resonator to align it with the wavelength of the incoming light. A refreshing pulse train has a lower optical power compared to that of a writing pulse. Hence, it cannot switch the ring resonator between two different states. The magnitude of a writing pulse, a refreshing pulse, and the required magnitude for optical switching are chosen based on the bistability response and the loss of the ring resonator, as shown in Fig. 2.

The optical memory unit is fabricated in the InP-InGaAsP material system. Figure 3 shows the experimental setup. A mode-locked laser (MLL) is used to generate the refreshing pulse train and the writing pulses. The MLL is locked to a microwave signal generator (SG) with an output frequency of 99.49 MHz. The MLL pulses are split by an optical coupler

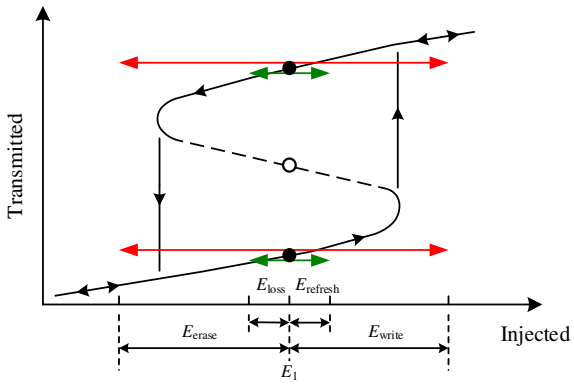

Fig. 2. Bistability response of the ring resonator from Port 1 to Port 2. The ring resonator has two possible output states at a given input of E_1. The refreshing pulse $E_{refresh}$ is used to compensate for the loss of the ring resonator within the refreshing period E_{loss}. Strong writing and erasing pulses are used to switch the ring resonator between two output states.

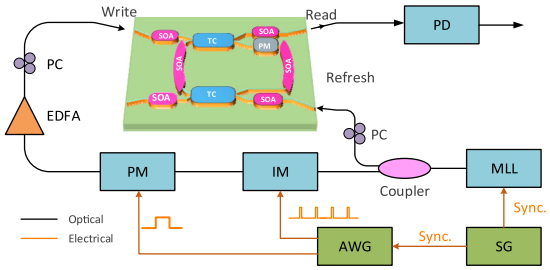

Fig. 3. Experimental setup. PD, photodetector; IM, intensity modulator; MLL, mode-locked laser; AWG, arbitrary waveform generator; SG, signal generator.

(OC), with one path directed to the refreshing port (Port 1) as the refreshing signal, and the other directed to an intensity modulator (IM) and a PM as a writing pulse with a phase of either "π" or "0." The writing pulse is amplified by an erbium-doped fiber amplifier before being injected into the memory unit via the writing port (Port 4). Two polarization controllers (PCs) are used to optimize the optical coupling to the chip. A two-channel electrical arbitrary waveform generator (AWG) synchronized to the SG is used to generate two rectangular waveforms that are applied to the IM and the PM. The rectangular waveform applied to the IM has a repetition rate of 9.949 MHz and a duty cycle of 10%. The rectangular waveform applied to the PM has a duty cycle of 50% and a repetition rate of 2.487 MHz. The joint operation of the IM and the PM results in a writing pulse train with a repetition time of 100.5 ns and a π phase shift every two pulses. Figure 4 shows the pulse train from the MLL and the electrical waveforms that are applied to the IM and the PM.

To obtain a long memory time, it is critical to ensure that the second refreshing pulse is injected into the ring resonator before the first refreshing pulse fully decays. This can be achieved either by minimizing the round-trip loss or increasing the repetition rate of the refreshing pulse train. The round-trip loss is estimated to be 3.6 dB, excluding the coupling ratio of

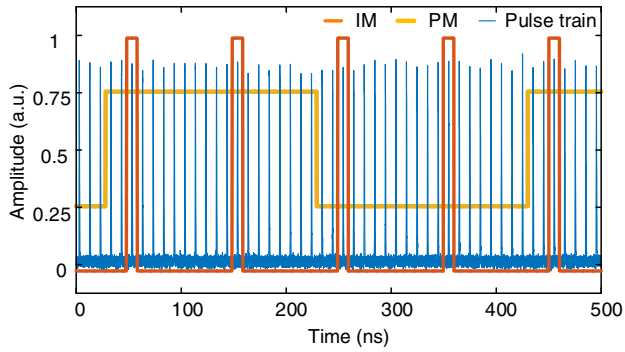

Fig. 4. Pulse train from the MLL fed to the refreshing port and the electrical signals applied to the IM and the PM.

the TCs. The two SOAs in the ring resonator can provide up to 20 dB of optical gain and, thus, can fully compensate for the round-trip loss. The optimum driving currents to the SOAs are chosen based on the coupling ratios of the TCs, and the net round-trip gain is kept below unity to avoid lasing. We first investigate the injection-power-dependent spectral response of the ring resonator. A continuous-wave light with a central wavelength at 1560 nm is launched into the memory via the refreshing port. As shown in Fig. 5(a), the measured resonance wavelength is redshifted by 15 pm when a light with a power of 16 dBm is injected. The wavelength shift is linearly proportional to the power increase.

Then we keep a constant injection power of 16 dBm and sweep the injection wavelength from 1559.79 to 1560.08 nm, as shown in Fig. 5(b). The resonance wavelength of the ring resonator is at around 1560.04 nm, and the FSR is around 218 pm. For the off-resonance injection wavelength from 1559.86 to 1559.99 nm, the resonance wavelength of the ring resonator does not change significantly. However, when a near-resonance wavelength from 1560.01 to 1560.03 nm is injected, the resonance wavelength is shifted dramatically and the peak of the spectral response drops, which agrees well with the prediction given by Eq. (3). The drop in the resonance peak is due to the saturation of the output SOA2 caused by the injected light. Thus, both the refractive index and the loss of the ring resonator are intensity dependent. Figure 5(a) shows a weaker nonlinearity within the ring resonator as compared with the case in Fig. 5(b), where the injection wavelength in Fig. 5(a) is far from the resonance wavelength which results in lower optical power confined in the ring resonator. An optical vector analyzer (OVA) is used to measure the transmission spectrum. Note that the power of the probe light from the OVA is low, so that no asymmetric spectral response with the resonance peak is seen.

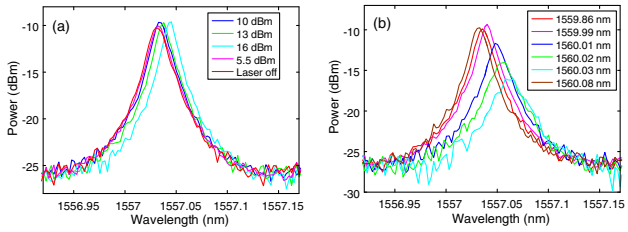

Fig. 5. Response of the ring resonator as a function of (a) the injecting optical power and (b) the injecting optical wavelength.

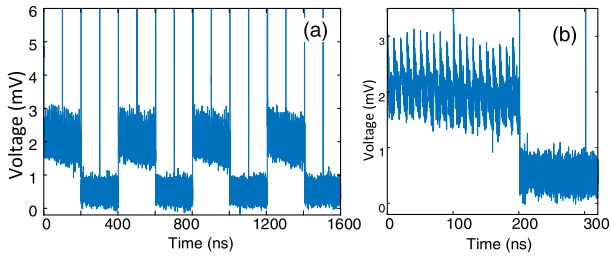

Fig. 6. (a) Detected waveform at the reading port when the writing and refreshing pulse trains illustrated in Fig. 4 are launched into the memory unit; (b) the zoom-in view of the waveform.

Then the ring resonator is tested as an optical memory. The bias current to the PM is tuned to find the optimum resonance wavelength corresponding to the central wavelength of the input optical signal. An optical writing pulse train with a periodic phase pattern of ["0", "0", "π", "π"] and a refreshing pulse train with a repetition rate of 99.49 MHz are launched into the memory via the writing port and the refreshing port, respectively. The optical signal obtained at the reading port is sent to a photodetector (PD) and sampled by an electrical oscilloscope. Figure 6 shows the sampled waveform. The memory is originally in the "0" state. No optical power can be detected at the PD, as the optical pulses coming from the refreshing port are off-resonance and blocked by the ring resonator. When a negative pulse with π phase is injected as the writing signal, the ring resonator will be shortly excited to have highly confined optical power. However, the optical signal confined in the ring resonator cannot be refreshed by the refreshing pulse train, as they are of opposite phases. In contrast, when a positive writing pulse is injected, the ring resonator will be excited by the confined signal having the same phase with the refreshing signal. The memory is then repeatedly refreshed and, eventually, reaches a stable state where the refreshing power perfectly compensates for the loss of the ring resonator. The ring resonator is then switched to and held at the high-level state representing an optical logic "1." To erase the stored optical information, a negative writing pulse with a phase of π is injected via the writing port. Destructive interference will occur so that the confined optical power goes below the bistability region, as indicated in Fig. 2. The memory returns to the low level state corresponding to an optical logic of "0." A memory time of 100 ns is achieved, as shown in Fig. 6. In fact, the memory time of the ring resonator can be infinite, if the phase coherence between two consecutive pulses from the MLL is preserved, so that the latter can refresh the former. The experimental writing and reading speed is 2.5 GHz, which is determined by the MLL pulse width of 0.4 ns. Note that the nonlinearity excitation time is in the scale of picoseconds [18], and the ring resonator has an FSR of 27.3 GHz, which indicates that the acceptable pulse can be as short as 36.6 ps or a writing and reading speed of 27.3 GHz, exceeding the speed of any state-of-the-art electronic dynamic random-access memory units. If a ring resonator with a smaller size is used, the writing and reading speed can be further increased.

The power consumption of the memory is mainly from the power consumption due to the electrical bias to SOA5 and due to the optical pulses to refresh the memory, which are calculated to be 72.86 mW and 100 dBm, respectively. We believe that the total power consumption can be reduced to be below 100 mW if the fiber-to-chip coupling loss and the round-trip loss are minimized.

In summary, an optically refreshable optical dynamic memory based on an active ring resonator was designed, fabricated, and demonstrated. A memory time of 100.5 ns was demonstrated by refreshing the optical memory every 10.05 ns. An infinite memory time can be potentially achieved if a refreshing signal is injected constantly. In our demonstration, the writing and reading speed was 2.5 GHz. It should be noted that the writing and reading speed can be increased by using pulses with a narrower temporal width to write, read, and refresh the memory. The proposed optical memory is suitable for large-scale integration to achieve a high-speed and large-capacity optical dynamic random-access memory array, in which ring resonators with different diameters can be constructed to realize wavelength-multiplexed optical memory. The proposed device eliminates the bottleneck of limited memory time of an optical memory based on a high Q resonator and reduces the complexity by using optical refresh and, thus, can find applications for future high-speed all-optical computation.

Funding. Natural Sciences and Engineering Research Council of Canada (NSERC).

REFERENCES

1. A. E. Willner, S. Khaleghi, M. R. Chitgarha, and O. F. Yilmaz, J. Lightwave Technol. **32**, 660 (2014).
2. W. Liu, M. Li, R. S. Guzzon, E. J. Norberg, J. S. Parker, M. Lu, L. A. Coldren, and J. Yao, Nat. Photonics **10**, 190 (2016).
3. T. D. Milster, Opt. Photon. News **16**(3), 28 (2005).
4. E. Walker and P. M. Rentzepis, Nat. Photonics **2**, 406 (2008).
5. M. Gu, X. Li, and Y. Cao, Light: Sci. Appl. **3**, e177 (2014).
6. X. Li, Y. Cao, N. Tian, L. Fu, and M. Gu, Optica **2**, 567 (2015).
7. W. Liu, M. Li, R. S. Guzzon, E. J. Norberg, J. S. Parker, L. A. Coldren, and J. Yao, J. Lightwave Technol. **32**, 3654 (2014).
8. T. Zhong, J. M. Kindem, J. Rochman, E. Miyazono, A. Faraon, A. Ferrier, and P. Goldner, Proc. SPIE **9762**, 97620J (2016).
9. E. Miyazono, I. Craiciu, A. Arbabi, T. Zhong, and A. Faraon, Opt. Express **25**, 2863 (2017).
10. R. W. Boyd, *Handbook of Laser Technology and Applications (Three-Volume Set)* (Taylor & Francis, 2003), pp. 161–183.
11. B. S. Wherrett, Appl. Opt. **24**, 2876 (1985).
12. S. Smith, I. Janossy, H. MacKenzie, J. Mathew, J. Reid, M. Taghizadeh, F. Tooley, and A. Walker, Opt. Eng. **24**, 244569 (1985).
13. M. T. Hill, H. J. Dorren, T. De Vries, X. J. Leijtens, J. H. Den Besten, B. Smalbrugge, Y.-S. Oei, H. Binsma, G.-D. Khoe, and M. K. Smit, Nature **432**, 206 (2004).
14. T. Christopoulos, O. Tsilipakos, and E. E. Kriezis, J. Appl. Phys. **122**, 233101 (2017).
15. M. Ferrera, Y. Park, L. Razzari, B. E. Little, S. T. Chu, R. Morandotti, D. Moss, and J. Azaña, Nat. Commun. **1**, 29 (2010).
16. L. Chrostowski and M. Hochberg, *Silicon Photonics Design: From Devices to Systems* (Cambridge University, 2015).
17. W. Zhang, W. Li, and J. Yao, Opt. Lett. **41**, 2474 (2016).
18. H. Wang, K. Ferrio, D. G. Steel, Y. Z. Hu, R. Binder, and S. W. Koch, Phys. Rev. Lett. **71**, 1261 (1993).